Spectroscopic determination of kinetic parameters for frequency sweeping Alfvén eigenmodes

Maxime Lesur, Y. Idomura, K. Shinohara, X. Garbet

Spectroscopic determination of kinetic parameters for frequency sweeping Alfvén eigenmodes

M. Lesur,[1,2] Y. Idomura,[1] K. Shinohara,[3] X. Garbet,[2] and the JT-60 Team[3]
[1]*Japan Atomic Energy Agency, Higashi-Ueno 6-9-3, Taitou, Tokyo 110-0015, Japan*
[2]*IRFM, Commissariat à l'Energie Atomique, F-13108 Saint Paul Lez Durance, France*
[3]*Japan Atomic Energy Agency, Mukouyama 801-1, Naka, Ibaraki 311-0193, Japan*

(Received 29 March 2010; accepted 21 September 2010; published online 17 December 2010)

A method for analyzing fundamental kinetic plasma parameters, such as linear drive and external damping rate, based on experimental observations of chirping Alfvén eigenmodes, is presented. The method, which relies on new semiempirical laws for nonlinear chirping characteristics, consists of fitting procedures between the so-called Berk–Breizman model and the experiment in a quasiperiodic chirping regime. This approach is applied to the toroidicity induced Alfvén eigenmode (TAE) on JT-60 Upgrade (JT-60U) [N. Oyama *et al.*, Nucl. Fusion **49**, 104007 (2009)], which yields an estimation of the kinetic parameters and suggests the existence of TAEs far from marginal stability. Two collision models are considered, and it is shown that dynamical friction and velocity-space diffusion are essential to reproduce nonlinear features observed in experiments. The results are validated by recovering measured growth and decay of perturbation amplitude and by estimating collision frequencies from experimental equilibrium data. © *2010 American Institute of Physics*. [doi:10.1063/1.3500224]

I. INTRODUCTION

In an ignited tokamak, the confinement of α-particles is critical to prevent damages on the first wall and to achieve break even. A major concern is that high energy ions can excite plasma instabilities in the frequency range of Alfvén eigenmodes (AEs), which significantly enhance their transport. Ever since the recognition of this issue in the 1970s, considerable progress has been made in the theoretical understanding of the principal Alfvénic instabilities. However, the estimation of the mode growth rate γ is complex, and the question of their stability in ITER (Ref. 1) remains to be clarified. Linear theory predicts that the toroidicity induced Alfvén eigenmode[2] (TAE) is stable when the continuous damping of the background plasma exceeds the drive of fast particles. Thus, accurate estimations of fundamental kinetic parameters such as the linear drive γ_L and the damping rate γ_d are needed, especially if the system is close to marginal stability, where γ is sensitive to small variations. For this class of instabilities, the growth rate can be estimated either by linear stability codes such as PENN,[3] TASK/WM,[4] NOVA-K,[5] or CASTOR-K (Ref. 6) or by gyrokinetic or drift-kinetic perturbative nonlinear initial value codes such as FAC (Ref. 7) or HAGIS.[8] The analysis requires internal diagnostics that are not always available. The global damping involves complicated mechanisms with details still under debate. Experimentally, γ_d can be estimated by active measurements of externally injected perturbations.[9,10] However, the applicability of this technique is limited to dedicated experiments, and this prevents robust linear predictions of the stability of AEs. Moreover, the existence of unstable AEs in a regime where linear theory predicts $\gamma<0$, or subcritical AEs, has not been ruled out. Therefore, nonlinear analysis is needed to assess the stability.

In general, these instabilities are described in a three-dimensional (3D) configuration space. However, near the resonant surface, it is possible to obtain a new set of variables in which the plasma is described by a one-dimensional (1D) Hamiltonian in two conjugated variables[11–14] if we assume an isolated single resonance. In this sense, the problem of AEs is homothetic to a simple 1D single mode bump-on-tail instability. The so-called Berk–Breizman (BB) problem[11,12,15] is a generalization of the bump-on-tail problem, where we take into account an external wave damping accounting for background dissipative mechanisms at a rate γ_d and a collision operator. Observed quantitative similarities between BB nonlinear theory and both global TAE simulations[13,16] and experiments[17,18] are an indication of the validity of this reduction of dimensionality.

A feature of the nonlinear evolution of AEs, the frequency sweeping (chirping) of the resonant frequency by 10%–30% on a timescale much faster than the equilibrium evolution, has been observed in the plasma core region of tokamaks JT-60U,[19] DIII-D,[20] the Small Tight Aspect Ratio Tokamak,[21] the Mega Amp Spherical Tokamak (MAST),[16] and the National Spherical Torus Experiment[22] and in stellerators such as the Compact Helical Stellerator,[23] and the Large Helical Device.[24] In general, two branches coexist, with their frequency sweeping downwardly (down-chirping) for one, upwardly (up-chirping) for the other. In most of the experiments, chirping events are quasiperiodic, with a period of the order of a millisecond. In many experiments, asymmetric chirping has been observed, with the amplitude of down-chirping branches significantly dominating up-chirping ones.

Qualitatively similar chirping modes are spontaneously generated by the BB model, and theory relates the time evolution of the frequency shift with γ_L and γ_d.[25] In this work, we identify a regime where chirping events are quasiperiodi-

cal. This regime exists whether the collision model is annihilation/creation type or takes into account dynamical friction and velocity-space diffusion. We recall the equations of the BB model and numerically investigate nonlinear chirping features for both collision operators in Sec. II. In a previous work,[26] we showed that the nonlinear time evolution of chirping in 1D simulations can be used to retrieve fundamental kinetic parameters with a good precision, which suggests that it is possible to retrieve kinetic parameters from experimental observations of chirping AEs. We propose a new method to estimate γ_L, γ_d, γ, and collision frequencies from the spectrogram of magnetic field variations measured by a Mirnov coil at the edge of the plasma. This method, which relies on a fitting of normalized chirping characteristics between the experiment and BB simulations, is described and applied to JT-60U AE experiments in Sec. III. We show that the BB model can successfully reproduce features observed in the experiment only if the collision operator includes drag and diffusion terms. In Sec. IV, an independent estimation of collision frequencies is obtained from experimental equilibrium measurements, and compared with the values obtained with our fitting procedure.

II. NONLINEAR FREQUENCY SWEEPING

A. The Berk–Breizman model

We adopt a perturbative approach and cast the so-called BB model[27] in a reduced form that describes the time evolution of the beam particles only.[28] The main hypothesis of this model is that the bulk particles interact adiabatically with the wave so that their contribution to the Lagrangian can be expressed as a part of the electric field. In this model, the real frequency of the wave is imposed as $\omega=\omega_p$, where $\omega_p \equiv (4\pi n_0 q^2/m)^{1/2}$ is the plasma frequency (in cgs units), q and m are the electronic charge and mass, and n_0 is the total plasma density. The evolution of the beam distribution, $f(x,v,t)$, is given by the kinetic equation

$$\frac{\partial f}{\partial t} + v\frac{\partial f}{\partial x} + \frac{q\tilde{E}}{m}\frac{\partial f}{\partial v} = \mathcal{C}(f-f_0), \tag{1}$$

where $\mathcal{C}(f-f_0)$ is a collision operator described below, $f_0(v)$ is the initial distribution function, and the pseudoelectric field $\tilde{E}$ is defined as

$$\tilde{E}(x,t) \equiv \frac{m}{q}[Q(t)\cos(\xi) - P(t)\sin(\xi)], \tag{2}$$

where $\xi \equiv kx - \omega_p t$.

In the definition of $\tilde{E}$, we assume a single mode of wave number k, reflecting the situation of a low toroidal mode number Alfvèn eigenmode, whose excited spectrum is usually discrete. The evolution of the pseudoelectric field is given by

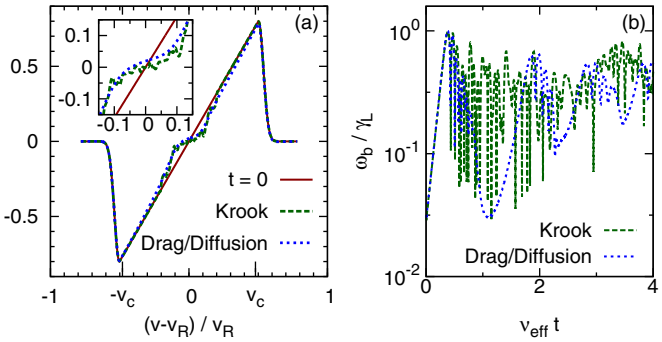

FIG. 1. (Color online) (a) Distribution function normalized to $n_0\gamma_{L0}/(\sqrt{2\pi}v_R\omega_p)$. Solid line is the initial condition, dashed lines are for $\nu_{\text{eff}}t=2$. (b) Time evolution of the bounce frequency. Parameters are $\gamma_{L0}=0.1$, $\gamma_d=0.05$, and $\nu_{\text{eff}}=0.02$. In the drag/diffusion case, $\nu_d/\nu_f=3$.

$$\frac{dQ}{dt} = -\frac{\omega_p^3}{2\pi n_0}\int f(x,v,t)\cos(\xi)dxdv - \gamma_d Q, \tag{3}$$

$$\frac{dP}{dt} = \frac{\omega_p^3}{2\pi n_0}\int f(x,v,t)\sin(\xi)dxdv - \gamma_d P, \tag{4}$$

where an external wave damping has been added to model all linear dissipation mechanisms of the wave energy to the background plasma, which are not included in the previous equations. In the initial condition, we apply a small perturbation, $f(x,v,t=0)=f_0(v)(1+\epsilon\cos kx)$, and the initial values of Q and P are given by solving the Poisson equation. We refer to Eqs. (1)–(4) as the δf BB model, in opposition to the full-f BB model studied in Ref. 26.

We define ω and γ as the real frequency and linear growth rate of the wave, respectively, including contributions of external damping and collisions. In the collisionless case, one can see from the linear dispersion relation that $\omega=\omega_p$ only if f_0 is symmetric around the resonant velocity, $v_R \equiv \omega/k$. Since we assumed $\omega=\omega_p$ from the start, we consider only such distributions, for the model to be self-consistent. The velocity distribution of beam particles in the initial condition, f_0, is shown in Fig. 1(a) for typical simulation parameters. A constant slope is imposed between $v=-v_c$ and $v=v_c$. The zero average ensures that the plasma frequency is not perturbed by the beam density. Smooth joins between the constant gradient region and the large velocity regions are necessary to prevent numerical oscillations at $v \approx \pm v_c$. For $\gamma/\omega \ll 1$, the dispersion relation yields

$$\gamma = \gamma_{L0} - \gamma_d, \tag{5}$$

where

$$\gamma_{L0} \equiv \frac{\pi}{2n_0}\frac{\omega_p^3}{k^2}\left.\frac{\partial f_0}{\partial v}\right|_{v=v_R}. \tag{6}$$

Let us define γ_L as the linear growth rate in the absence of collisions and external dissipation. Note that in general, γ_{L0} and γ_L are slightly different. In this paper, we use γ_{L0} solely as a measure of the slope of the initial velocity distribution.

We consider two collision models. On the one hand, a large part of existing theory takes into account collisions in the form of a Krook operator,[29]

$$\mathcal{C}_K(f-f_0) = -\nu_a(f-f_0), \tag{7}$$

which is a simple model for collisional processes that tend to recover the initial distribution at a rate ν_a, including both source and sink of energetic particles. On the other hand, a more realistic collision operator, the one-dimensional projection of a Fokker–Plank operator,[30] includes a dynamical friction (drag) term and a velocity-space diffusion term,

$$\mathcal{C}_{FP}(f-f_0) = \frac{\nu_f^2}{k}\frac{\partial(f-f_0)}{\partial v} + \frac{\nu_d^3}{k^2}\frac{\partial^2(f-f_0)}{\partial v^2}. \tag{8}$$

Another large part of existing theory deals with the latter operator in the absence of drag ($\nu_f=0$). Investigations of the effects of dynamical friction are fairly recent.[30] We define the effective collision frequency as $\nu_{\text{eff}} \equiv \nu_a$ in the Krook case and $\nu_{\text{eff}} \equiv \nu_d^3/\gamma_{L0}^2$ in the case with diffusion.

In a previous work,[26] we developed and validated a 1D semi-Lagrangian Vlasov code, referred to as COBBLES, including a Krook operator and extrinsic dissipation, capable of long-time, accurate nonlinear simulations of both full-f and δf BB models. In this paper, we use the δf version of COBBLES to investigate the nonlinear characteristics of chirping solutions. For this work, a collision operator with drag and diffusion is implemented. We confirmed quantitative agreement of nonlinear steady-state solutions between the extended code and Ref. 30. Detailed verification will be included in a separate publication. Both in our simulations and in the remainder of this paper, time is normalized to ω_p unless some physical unit is explicitly given. When we compare simulation and experimental results, we simply renormalize time by the measured AE linear frequency. In this work, all simulations are performed with $N_x \times N_v = 64 \times 2048$ grid points and a time-step width 0.05. The large number of grid points in velocity space is necessary to avoid recurrence effect during the quiescent phase between two chirping events.

B. Chirping characteristics

The nonlinear behavior of an instability is determined by a competition among the drive by resonant particles, the external damping, the particle relaxation that tends to recover the initial positive slope in the distribution function, and particle trapping that tends to smooth it. Chirping solutions arise in a low collision regime when hole and clump structures[11] are formed in phase-space. They belong to a chaotic regime, and each chirping event is slightly different. The velocity distribution after nonlinear saturation shown in Fig. 1(a) illustrates the fact that several holes and clumps with different amplitudes can coexist. In this work, we are interested in the nonlinear chirping characteristics, averaged over a significant number of chirping events. In particular, in our simulations, the first chirping event is observed to stand out from the statistics, with a larger extent of chirping—up to twice as much as any other one of the following series of repetitive chirping. This may be due to the fact that the first chirping benefits from a perfectly constant velocity-slope, while following events are subject to the interference of phase-space structures that remain from previous chirping events. Since the latter condition seems more experimentally relevant, the first chirping is ignored in the present analysis.

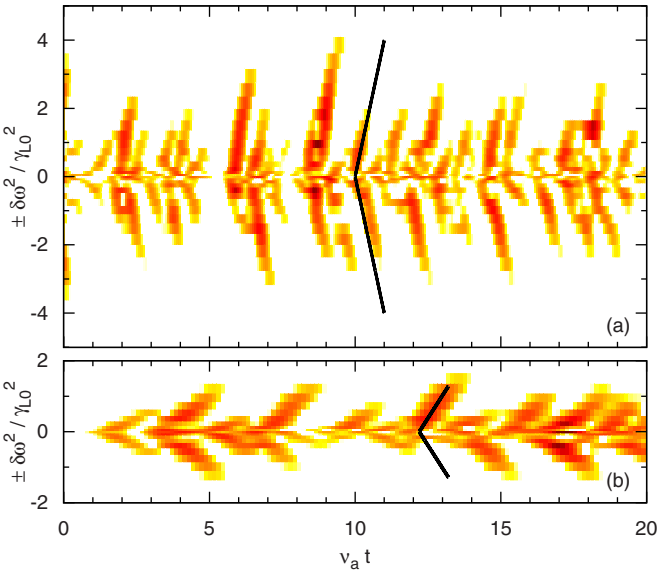

FIG. 2. (Color online) Spectrogram of the electric field, obtained with a moving Fourier window of size 510 for $\gamma_{L0}=0.1$ and (a) $\gamma_d=0.04$, $\gamma_d\nu_a/\gamma_{L0}^2=0.008$, and $\beta=1.0$; (b) $\gamma_d=0.09$, $\gamma_d\nu_a/\gamma_{L0}^2=0.043$, and $\beta=0.57$. Solid lines show the chirping velocity predicted by Eq. (9), with the correction coefficient β, and the chirping lifetime predicted by Eq. (12). Throughout this paper, the logarithmic color scale for each spectrogram spans three orders of magnitude.

Reference 25 shows how one can isolate one spectral component and model it by a Bernstein–Greene–Kruskal wave[31] to obtain the time evolution of one chirping event. In a regime where $\dot{\delta\omega}/\omega_b^2$, $\ddot{\delta\omega}/\omega_b^3$, $\dot{\omega}_b/\omega_b^2$, and $\omega_b/\delta\omega \ll 1$, the perturbation of the passing particle distribution is negligible, and a bounce average of the trapped particle distribution yields the frequency shift, in the collisionless limit, as

$$\delta\omega(t) = \alpha\gamma_{L0}\sqrt{\gamma_d t}, \tag{9}$$

with $\alpha \approx 0.44$, and a saturation level as

$$\omega_b \approx 0.54\gamma_{L0}, \tag{10}$$

where the bounce frequency ω_b of particles that are deeply trapped in the electrostatic potential, defined here as $\omega_b^4 \equiv k^2(Q^2+P^2)$, is used as a measure of the electric field amplitude. These analytic expressions have been found to agree with 1D simulations of both δf and full-f BB model,[25,26] with both Krook and diffusion-only collision operators, and with 3D HAGIS simulations.[16] Figure 2(a) shows the spectrogram of a chirping solution in the aforementioned regime. In Sec. III, we consider frequency sweeping in a regime where $\dot{\delta\omega}/\omega_b^2 \approx 0.5$, which approaches the limit of validity of the above theory. $\dot{\delta\omega}/\omega_b^2$ can be seen as a measure of the hole/clump adiabaticity, and is roughly proportional to $(\gamma_d\nu_a)^{1/2}/\gamma_{L0}$ in the Krook case. When $\dot{\delta\omega}/\omega_b^2 \approx 0.5$, $4\omega_b/\dot{\delta\omega} \approx 2\pi/\omega_b$; in other words, a hole or a clump is shifted by its width in a bounce time of deeply trapped particles. In this regime, the previous analytic treatment is not relevant. However, numerical simulations show a similar square-root dependency of the frequency shift in time. We

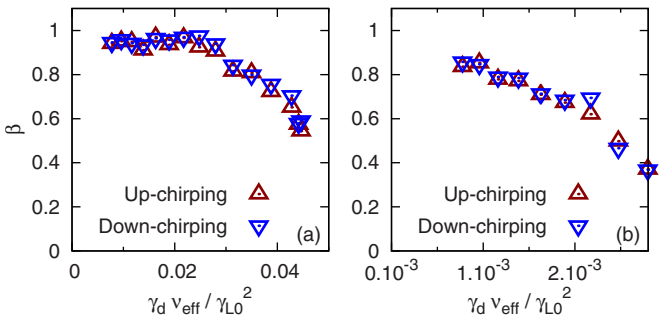

FIG. 3. (Color online) Correction to Eq. (9) when the timescale of frequency shift is relatively short compared to the bounce period, for $\gamma_{L0}=0.1$. The ratio $\gamma_d/\nu_{\rm eff}$ is such that $\delta\omega(1/\nu_{\rm eff})=0.2$ in Eq. (9). (a) In the Krook case, spectrograms for two extreme points are shown in Fig. 2. (b) With drag and diffusion, $\nu_d/\nu_f=10$.

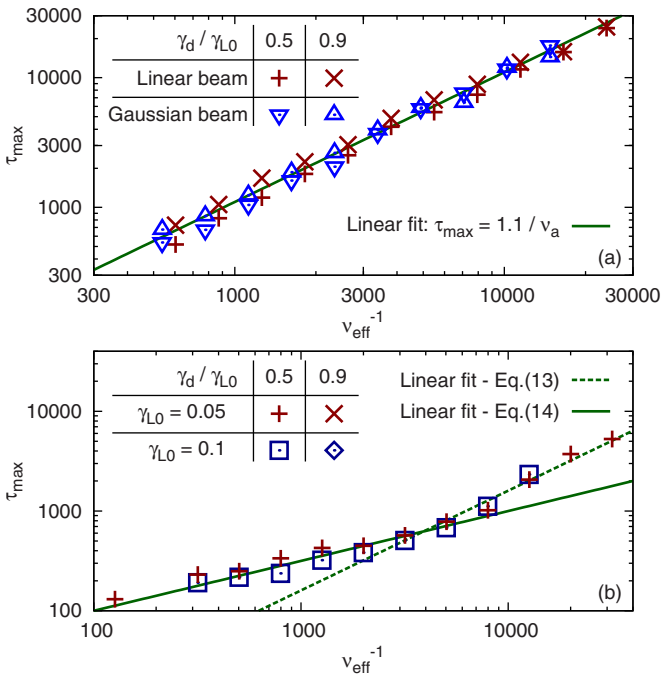

FIG. 4. (Color online) Maximum lifetime of a hole or clump, far from marginal stability, $\gamma_d/\gamma_{L0}=0.5$, and near marginal stability, $\gamma_d/\gamma_{L0}=0.9$. (a) With a Krook collision operator. The crosses correspond to the initial distribution shown in Fig. 1(a), while the triangles correspond to a bump-on-tail distribution with a Gaussian beam. In both cases, $\gamma_{L0}=0.05$. The solid line corresponds to Eq. (12). (b) With a diffusive collision operator (for a linear distribution only) for two different values of linear drive. The dashed line corresponds to Eq. (13) with $\iota_d=0.16$, and the solid line corresponds to Eq. (14) with $\iota_d=10$. The drag is chosen so that it does not significantly alter the chirping lifetime, $\nu_d/\nu_f=10$. An absence of points means that we do not observe repetitive chirping before the end of the simulation ($t=100\,000$).

introduce the effect of nonadiabaticity on chirping velocity as a correction parameter β, defined as

$$\beta \equiv \frac{\delta\omega(t)}{\alpha\gamma_{L0}\sqrt{\gamma_d t}}. \tag{11}$$

β is obtained numerically for $\gamma_{L0}/\omega=0.1$ in Fig. 3. We confirm that inside the validity limit of the above theory, β approaches unity. Even for relatively large values of $\delta\omega/\omega_b^2$, the chirping velocity has a smooth dependency on the kinetic parameters. The latter point is crucial for the validity of the procedure described in Sec. III. The spectrograms corresponding to the two extreme points of Fig. 3(a) are shown in Fig. 2.

The resonant velocity of a hole (a clump) does not increase (decrease) indefinitely. We define the lifetime τ of a chirping event as the time it takes to the corresponding power in the spectrogram to decay below a fraction e^{-2} of the maximum amplitude reached during this chirping event. The maximum lifetime $\tau_{\rm max}$ is the maximum reached by τ during a time-series, ignoring the first chirping event and any minor event. It is reasonable to assume that the island structure is dissipated by collisional processes, in which case the maximum chirping lifetime should be of the form

$$\tau_{\rm max} = \frac{\iota_a}{\nu_a}, \tag{12}$$

in the Krook case, and

$$\tau_{\rm max} = \iota_d \frac{\gamma_{L0}^2}{\nu_d^3}, \tag{13}$$

in the case with drag and diffusion when $\nu_f \ll \nu_d$, where ι_a and ι_d are constant parameters. In Fig. 4, we plot the maximum lifetime measured in COBBLES simulations where the ratio γ_d/γ_{L0} is chosen as 0.5 and 0.9, i.e., far from and close to marginal stability, respectively. A quantitative agreement is found with Eq. (12), with $\iota_a=1.1$, for ν_a^{-1} spanning two orders of magnitude. With the diffusive collision operator, the chirping lifetime agrees with Eq. (13) only for low collisionality. For high collisionality, diffusion affects the width of a hole or clump during the first phase of their evolution, namely, drive by free-energy extraction, which in turn affects the decay by diffusion. Since chirping observed in experiments has a lifetime of the order of $\tau\sim 500$, we adopt a semiempirical law obtained by a linear fit,

$$\tau_{\rm max} = \iota_d \left(\frac{\gamma_{L0}^2}{\nu_d^3}\right)^{0.5}, \tag{14}$$

with $\iota_d=10$. No repetitive chirping is found near marginal stability for $0.05 \le \gamma_{L0} \le 0.1$, though longer computations may reveal this possibility.

In the following analysis of TAE experiments, Eqs. (12) and (14) are used as diagnostics for the effective collision frequency; thus, it is important that these results are not too sensitive to the shape of the fast particles distribution. To investigate this point, we repeat the same analysis (in the Krook case), this time with an initial bump-on-tail distribution with a Gaussian beam instead of a constant gradient, or linear, beam. Figure 4(a) shows that the agreement is kept, even if the shape of the distribution has a significant effect on the extent of chirping as can be seen for example in Fig. 12 of Ref. 26.

As long as the background plasma parameters are not significantly changed, chirping events in most tokamak experiments are quasiperiodic, with a quiescent phase between two chirping branches that lasts a few milliseconds. It should be noted that this statement does not seem to apply to DIII-D.[20] In some parameter regimes, the chirping arising

from the BB model with Krook collisions is also quasiperiodic, although the phase between two major chirping events is generally not as quiet as in the experiments. In a regime where $\nu_f \ll \nu_d$, the chirping arising from the BB model with drag and diffusive collisions is quasiperiodic too, but this time with clear quiescent phases in-between chirping events. In Fig. 1(b), which shows periodic decay and recovery of perturbation amplitude, corresponding to major chirping events, we observe qualitatively different behavior between the two collision models. In both case, no analytic theory has been developed to predict the average time between two chirping events, Δt_{chirp}. However, conceptually, there exists some relation with a subset of the input parameters. Thus, if we normalize time with the mode frequency, then chirping velocity, lifetime, and period are dictated by the input parameters of the model, γ_{L0}, γ_d, and ν_a, or ν_f and ν_d. In the Krook case, we have a three-variable, three-equation system, which we solve by a fitting procedure described in Sec. III. With drag and diffusion, there is one additional degree of freedom; hence, the solution is not unique, but the boundaries of chirping regime limit the possible range of input parameters.

III. ANALYSIS OF EXPERIMENTAL CHIRPING MODES

A. Fitting procedure

We consider magnetic field perturbations measured by a Mirnov coil at the edge of a fusion plasma, for a time interval during which quasiperiodic, perturbative chirping is observed, and during which background plasma parameters are not significantly changed, since a fixed mode structure is assumed to reduce the problem to a one dimensional Hamiltonian. We also assume that frequency shifting occurs well within the gap of the Alfvén continuum, so that chirping lifetime is determined by collision processes, rather than by continuum damping. In the corresponding magnetic spectrogram, we extract the linear mode frequency f_{A}, the average chirping velocity $d\delta\omega^2/dt$, the maximum chirping lifetime $\tau_{\max}$, and the average chirping period Δt_{chirp}. Equation (9) gives a relation between linear drive and external damping,

$$\gamma_{L0}^2 \gamma_d = \frac{1}{\alpha^2 \beta^2} \frac{d\delta\omega^2}{dt}. \tag{15}$$

With the Krook model, chirping is limited to a range where $0.2 < \gamma_d/\gamma_{L0} < 1.1$.[26] We found a similar constraint in our simulations with drag and diffusion, although a full scan of parameter space remains to be done. From this observation, in both cases, γ_{L0} is given within roughly 30% error, and γ_d within 50% error, by

$$\gamma_{L0} \approx 1.3 \left(\frac{1}{\alpha^2 \beta^2} \frac{d\delta\omega^2}{dt} \right)^{1/3}, \tag{16}$$

$$\gamma_d \approx 0.7 \left(\frac{1}{\alpha^2 \beta^2} \frac{d\delta\omega^2}{dt} \right)^{1/3}. \tag{17}$$

We refine these estimations in a manner that depends on the collision model we adopt.

1. With Krook collisions

The analysis described here aims at estimating the values of γ_{L0}, γ_d, and ν_a for which the δf BB model fits experimental observations in terms of chirping characteristics. Equation (12) yields the effective collision frequency,

$$\nu_a = \frac{\iota_a}{\tau_{\max}}. \tag{18}$$

Note that this effective collision frequency is meaningful only in the framework of a modelization by the simple Krook operator of all dissipative processes: particle collisions, particle source, and particle sink. Thus, this effective collision frequency ν_a cannot be quantitatively compared with experimental measurements of collision frequency unless particle source and sink terms are fully identified as well. Equations (15) and (18) form a system of two equations with three unknowns. The remaining unknown is found by fitting the chirping period. In our simulations, the chirping period is estimated by searching for the dominant frequency in the Fourier spectrum of the electric field amplitude. To ensure a reasonable accuracy, simulations are performed for a time $t \gg \Delta t_{\text{chirp}}$. If the experiment belongs to a regime where $\beta = 1$, the above procedure is systematic. However, if β is significantly smaller than unity, an iterative procedure is needed, with a feedback between β and $\gamma_{L0}^2 \gamma_d$.

2. With drag and diffusion

The analysis described here aims at estimating the values of γ_{L0}, γ_d, ν_f, and ν_d for which the δf BB model fits experimental observations. Equations (14) and (15) form a system of two equations with four unknowns. The boundaries of the chirping regime yield an estimation of ν_d within 20% error,

$$\nu_d \approx 1.2 \left(\frac{\iota_d}{\tau_{\max}} \right)^{2/3} \left(\frac{1}{\alpha^2 \beta^2} \frac{d\delta\omega^2}{dt} \right)^{2/9}. \tag{19}$$

On the one hand, it is shown in Ref. 30 that for typical neutral beam-heated experiments, the ratio ν_d/ν_f is of the order of unity. On the other hand, a numerical exploration of chirping regimes with drag and diffusion, which will be detailed in a future publication, suggests that when $\nu_f \geq \nu_d$, the drag significantly modifies the shape of chirping, to the point where we leave the regime of repetitive chirping. Thus, the relevant regime for friction is $\nu_f \lesssim \nu_d$. In this regime, Δt_{chirp} increases with decreasing ν_f and γ, and increasing ν_d. To refine the above estimations, and estimate ν_f, we need a two-dimensional scan in (ν_f, ν_d), where we search for solutions that fit the chirping period. In general, $\beta \neq 1$, and trial-and-errors are required to adjust the chirping velocity to the experimental value.

B. Application to JT-60U

In JT-60U, TAEs are destabilized by a negative ion based neutral beam (N-NB), which injects deuterons at $E_b = 360$ keV. A distinction is made between so-called abrupt large-amplitude events (ALEs) and fast frequency sweeping (fast-FS).[32] In this paper, we focus on the latter phenomenon, which has a timescale of 1–5 ms, and with which the asso-

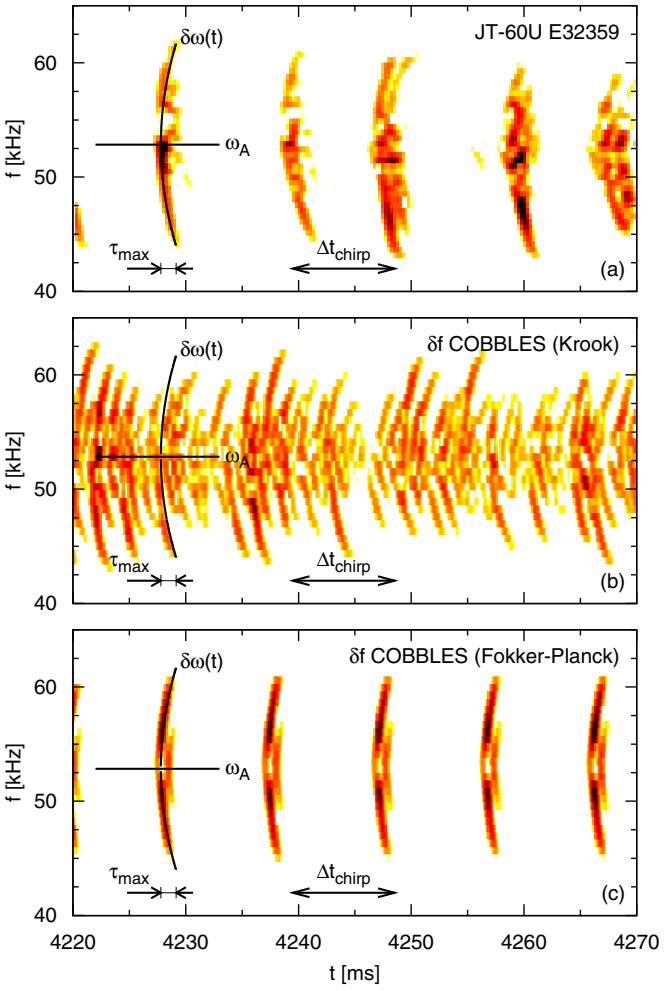

FIG. 5. (Color online) (a) Spectrogram of magnetic fluctuations during fast-FS modes in the JT-60U discharge E32359, obtained with a moving Fourier window of size 2 ms. [(b) and (c)] Spectrogram of the electric field where the kinetic parameters of the δf BB model were chosen to fit the magnetic spectrogram for JT-60U discharge E32359. The solid curve shows the analytic prediction for the chirping velocity. (b) Krook collisions, correction parameter $\beta=0.65$. (c) Friction-diffusion collisions, correction parameter $\beta=0.85$.

ciated redistribution of energetic ions is relatively small.[33] ALEs are identified as energetic particle driven modes,[34] have larger amplitude, shorter timescale (200–400 μs), induce significant loss of energetic ions, and are out of the scope of this work since we assume a constant density of energetic ions.

In the discharge E32359, around $t=4.2$ s, frequency sweeping modes have been identified as $m/n=2/1$ and 3/1 TAEs.[19] In the spectrogram shown in Fig. 5(a), we measure $f_A=53$ kHz, $d\delta\omega^2/dt=6.3\times10^{-5}$, $\tau_{max}=0.44\times10^3$, and $\Delta t_{chirp}=3\times10^3$ (on average).

1. With Krook collisions

Equations (15) and (18) yield $\nu_a=0.25\%$, and $\gamma_{L0}\sqrt{\gamma_d}=1.8\times10^{-2}$. However, the results of our analysis suggest that the plasma belongs to a regime where $\beta=0.65$, so we adjust the value of the product $\gamma_{L0}\sqrt{\gamma_d}$ to $1.8\times10^{-2}/0.65=2.8\times10^{-2}$.

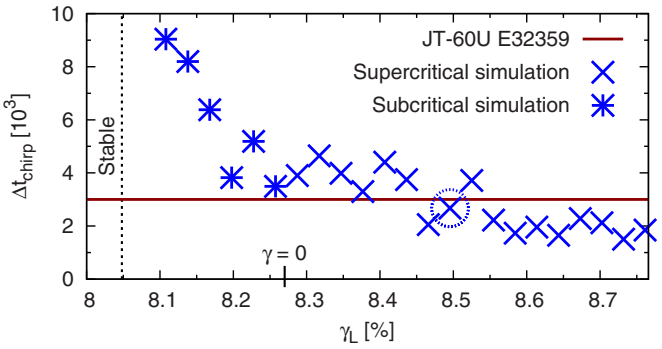

FIG. 6. (Color online) Scan of the chirping quasiperiod for the set of parameters corresponding to JT-60U discharge E32359. The region where $\gamma/\gamma_L>0.1$, where $\Delta t_{chirp}<2\times10^3$ is not included in this plot. Both linear and nonlinear stability thresholds are indicated. The chirping quasiperiod agrees with the experiment for $\gamma_L\approx8.5\%$. The spectrogram for the circled simulation is shown in Fig. 5(b).

A scan for this set of parameters is performed by changing the slope of the distribution. Figure 6 shows that the chirping quasiperiod depends on γ_L in a roughly monotonous way. Note that the scan needs to be performed on a relatively narrow range of the kinetic parameters, since the limits of subcritical regime and nonchirping (chaotic) regime yield a first estimate as $\gamma_L\sim8\%-12\%$ and $\gamma_d\sim4\%-10\%$, in percentage of the mode frequency $\omega_A=2\pi f_A$. Here, the nonlinear stability threshold is defined as the largest value of γ_L for which the electric field amplitude tends to zero in the time-asymptotic limit, independently of the initial perturbation amplitude; the chaotic regime is defined and categorized in a way described in Ref. 26. We observe that the two-point correlation of electric field amplitude decreases as the system approaches marginality.

Figure 5(b) is the spectrogram for the simulation which is emphasized by a circle in Fig. 6. The features of the main chirping events agree with the experimental observation. However, we observe a series of minor chirping events in between, which are absent from the experimental spectrogram. Another caveat is that only symmetric chirping is observed with the δf BB model with Krook collisions and a linear velocity distribution. Thus, the application of this method with Krook collisions is restricted to symmetric or nearly-symmetric chirping experiments. The linear parameters estimated from this analysis are shown in Table I. Our analysis suggests that the TAE in this discharge is marginally unstable, with $\gamma/\gamma_L\sim0.1$, even though $\gamma_L<\gamma_d$, which is not inconsistent with Eq. (5) since $\gamma_{L0}>\gamma_d$. However, these values are inconsistent with estimations that take into account drag and diffusion processes. Since the following analysis

TABLE I. Frequencies and growth rates estimated from the magnetic spectrogram of chirping TAEs, in percentage of the mode frequency $\omega_A=2\pi f_A$.

Collision model	γ_{L0} (%)	γ_L (%)	γ_d (%)	ν_a (%)	ν_f (%)	ν_d (%)	γ (%)
Krook	9.4	8.5	8.6	0.25	⋯	⋯	0.7
Fokker–Planck	9.8	9.2	4.7	⋯	0.36	1.7	4.6

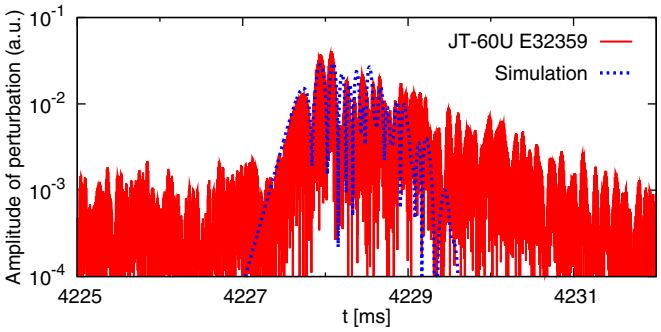

FIG. 7. (Color online) Evolution of the perturbation during a single chirping event. The signal is filtered between 40 and 65 kHz. In these arbitrary units, 10^{-3} roughly corresponds to a noise level. The parameters of the simulation are shown in Table I. For the simulation, to avoid hiding experimental data, we show the amplitude of perturbations instead of the perturbations themselves. Note the use of arbitrary units (we only compare normalized quantities).

shows much better agreement with the experiment, we imply that the Krook model is insufficient to describe nonlinear features related to repetition of chirping.

2. With drag and diffusion

We perform a first, rough scan in (ν_f, ν_d) parameter space, assuming $\beta=1$. Measuring average chirping velocity in repetitive chirping solutions yields an estimation of the correction parameter, $\beta=0.85$. Then Eqs. (16), (17), and (19) yield $\gamma_{L0}=10^{\pm 3}\%$, $\gamma_d=5^{\pm 3}\%$, and $\nu_d=1.7^{\pm 0.4}\%$. We perform a second, more careful scan, which consists of a series of 4×8 simulations in the domain $(1.5\% \le \nu_d \le 2.2\%$ and $1 \le \nu_d/\nu_f \le 8)$, where γ_{L0} and γ_d are constrained by Eqs. (14) and (15). The only repetitive chirping solution with $2500 < \Delta t_{\text{chirp}} < 3500$ we found is shown in Fig. 5(c). We verify that chirping features measured in this simulation, $d\delta\omega^2/dt = 7.1\times 10^{-5}$ (6.2×10^{-5} for up-chirping and 7.9×10^{-5} for down-chirping), $\tau_{\max}=0.45\times 10^3$ (0.47×10^3 for up-chirping and 0.43×10^3 for down-chirping), and $\Delta t_{\text{chirp}}=2.8\times 10^3$, fit the experiment. The estimated linear parameters are shown in Table I. In theory, the solution is not unique, but the latter estimations are quite accurate because of the narrow range of periodic chirping regime. To validate this analysis, we compare the amplitude of perturbations in Fig. 7. Since the growth rate of chirping structure is neither γ nor γ_L and the decay rate is not simply γ_d but a function of several linear parameters, the agreement we obtain is not trivial (we measure a growth rate of 2.3% and a decay rate of 0.3%). For further validation, we estimate the values of ν_f and ν_d from plasma parameters in Sec. IV.

IV. ESTIMATION OF COLLISION FREQUENCIES

A. Projection of Fokker–Planck collision operator

We consider collisions on energetic particles by thermal electrons $(s=e)$, ions $(s=i)$, and carbon impurities $(s=c)$ and describe them by a Fokker–Planck collision operator[35] that acts on the distribution $f(\boldsymbol{x},\boldsymbol{v},t)$ of energetic particles $(s=b)$. In spherical coordinates (v,Θ), neglecting gyroangle dependency,

$$\left.\frac{df}{dt}\right|_{\text{coll.}} = \nu_{\text{defl}}\frac{1}{2}\frac{1}{\sin\Theta}\frac{\partial}{\partial\Theta}\left(\sin\Theta\frac{\partial f}{\partial\Theta}\right) + \frac{1}{v^2}\frac{\partial}{\partial v}\left[v^3\left(\nu_{\text{slow}}f + \frac{1}{2}\nu_{\|}v\frac{\partial f}{\partial v}\right)\right], \tag{20}$$

where ν_{defl}, ν_{slow}, and $\nu_{\|}$ are pitch-angle scattering, slowing-down, and parallel velocity diffusion rates, respectively, $v_{\|} \equiv \boldsymbol{v}\cdot\boldsymbol{b} = v\cos\Theta$ is the parallel velocity of energetic particles, $\boldsymbol{b}\equiv\boldsymbol{B}_0/B_0$, and $\boldsymbol{B}_0$ is the equilibrium magnetic field.

We consider a TAE with toroidal mode number n, resulting from the coupling of m and $m+1$ poloidal modes. To simplify the following discussion, we consider strongly co-passing beam particles that resonate with the TAE at a velocity $v\approx v_{\|}=v_A$, where v_A is the Alfvén velocity. Then, the resonance condition is given by $\Omega=\omega_{\text{A}}$, where

$$\Omega = n_{\text{A}}\frac{v_{\|}}{R_0} - m\frac{v_{\|}}{q(r)R_0}, \tag{21}$$

R_0 is the major radius of the magnetic axis, $q(r)$ is the safety factor, and r is the minor radius. To project the Fokker–Planck operator on the resonant surface, we follow the procedure described in Refs. 11 and 30. We substitute $\partial_{\boldsymbol{v}}f$ by $\mathcal{J}\boldsymbol{b}\partial_\Omega f$, where P_ζ is the toroidal angular momentum,

$$P_\zeta \equiv -\frac{e_b}{c}\psi(r) + m_b R_0 v_{\|}, \tag{22}$$

$\mathcal{J}$ is the Jacobian of the coordinate transformation from $v_{\|}$ to Ω,

$$\mathcal{J} = \frac{\partial P_\zeta}{\partial v_{\|}}\left.\frac{\partial\Omega}{\partial P_\zeta}\right|_{v_{\|}} = \frac{mcSm_b v_{\|}}{2r^2 e_b B_0}, \tag{23}$$

and $S\equiv rq'/q$ is the magnetic shear. Here, e_s and m_s are charge and mass of a species s, respectively, and b stands for beam particles. This procedure yields

$$\left.\frac{df}{dt}\right|_{\text{coll.}} = \nu_f^2\frac{\partial f}{\partial\Omega} + \nu_d^3\frac{\partial^2 f}{\partial\Omega^2}, \tag{24}$$

with

$$\nu_f^2 = v_{\|}\mathcal{J}(2\nu_{\|} + \nu_{\text{slow}} - \nu_{\text{defl}}), \tag{25}$$

$$\nu_d^3 = \frac{v^2}{2}\mathcal{J}^2(\nu_{\|}\cos\Theta + \nu_{\text{defl}}\sin\Theta). \tag{26}$$

We assume Maxwellian background distributions with same temperature T_0. Typical experiments satisfy the following ordering of thermal velocities: $v_{Tc} < v_{Ti} \ll v_A \ll v_{Te}$, while the beam energy E_b is much larger than T_0. With these assumptions, around the resonance,

$$\nu_f^2 = \frac{v_\parallel \mathcal{J}}{v^3} \sum_s \frac{n_s \gamma_{bs}}{m_s} \left[\text{erf } \eta_s - \frac{2\eta_s}{\sqrt{\pi}} e^{-\eta_s^2} \right], \tag{27}$$

$$\nu_d^3 = \frac{\mathcal{J}^2}{2v^3} \sum_s \frac{n_s \gamma_{bs}}{2m_b \eta_s^2} \left\{ [(2\eta_s^2 - 1)v_\perp^2 + 2v_\parallel^2] \text{erf } \eta_s + \frac{2\eta_s}{\sqrt{\pi}} (v^2 - 3v_\parallel^2) e^{-\eta_s^2} \right\}, \tag{28}$$

where $\eta_s \equiv v/v_{Ts}$, $v_\parallel = v_A$,

$$\gamma_{bs} = \frac{4\pi e_b^2 e_s^2 \log \Lambda}{m_b}, \tag{29}$$

and $\log \Lambda$ is the Coulomb logarithm. Since the magnetic moment is an invariant of the motion of injected beam ions from deposition to resonant surface, $v_\perp^2 = v_b^2(1 - R_T^2/R_0^2)$, where v_b is the velocity of beam particles and R_T is the tangential radius of the beam. The equivalent collision operator in the Berk–Breizman model is obtained by substituting $\Omega = kv$ in Eq. (24).

B. Application to JT-60U

In the discharge E32359 around $t=4.2$ s, the resonant surface of the $m/n=2/1$ and 3/1 TAE is located around $r=0.7$ m. The magnetic shear is estimated from the q profile,[36] $S=0.8$. The deuteron plasma has the following characteristics: $B_0=1.2$ T, $R_0=3.3$ m, and the tangential radius of the N-NB is $R_T=2.6$ m. At $r=0.7$ m, $n_e=1.4\times10^{-19}$ m^{-3}, and $T_0=0.75$ keV. We take into account carbon impurities with $Z_{\text{eff}}=2.7$. With these equilibrium measurements, Eqs. (27) and (28) yield $\nu_f/\omega=1.2\%$ and $\nu_d/\omega=1.7\%$. Note that the electrons account for 99% of ν_f^2, which reflects a high Alfvén velocity, while impurities account for 57% of ν_d^3, which is consistent with the fact that pitch-angle scattering is more effective with heavier particles. The value of ν_d estimated in Sec. III B 2 quantitatively agrees with this independent estimation. However, with our fitting procedure, ν_f was underestimated by 70%. Though error bars in the experimental data may account for this discrepancy, it is also possible that our model misses some mechanism that would enhance the friction.

V. CONCLUSION

In the present study, we found a regime of quasiperiodic chirping with both Krook and Fokker–Planck collision operators. Since quantitative agreement with theory suggests the predictability of nonlinear chirping characteristics based on fundamental linear kinetic parameters, the latter may be estimated in the opposite way from chirping data in experiments. More precisely, chirping velocity and lifetime yield two relations among γ_L, γ_d, and collision frequencies, and a fitting of Δt_{chirp} yields an estimation of remaining unknowns. Note that major advantages of this technique are (1) kinetic parameters in the core of the plasma estimated only from the spectrogram of magnetic fluctuations measured at the edge, without expensive kinetic MHD calculations nor detailed core diagnostics, and (2) unified treatments of supercritical and subcritical AEs. We showed that drag and diffusion are essential to reproduce quiescent phases observed in experiments between chirping events. We confronted this procedure by analyzing AEs on JT-60U. We found quantitative agreement with measured magnetic fluctuations for the growth and decay of chirping structures and qualitative agreement with collision frequencies estimated from experimental background measurements. In these estimations, impurities, which were not included in estimations of Ref. 30, account for the main part of velocity diffusion. An effect of drag is to break the symmetry around the resonant velocity. The discrepancy between simulations and experiments in terms of asymmetry between up-shifting and down-shifting frequencies remains to be clarified. Preliminary results show that the shape of the energetic particle distribution has a significant effect on chirping asymmetry. In the present analysis, we chose a linear initial distribution. However, it is unclear what shape of velocity distribution is relevant to the experiment. Many experiments in JT-60U and MAST feature repetitive chirping with velocity, lifetime, and period comparable to the TAE analyzed here, and we plan to apply the same procedure to these data in order to survey the dependency of kinetic parameters on fundamental plasma parameters. Finally, we will work toward an analytic theory for the chirping quasiperiod, or an empirical formula, which would improve the robustness of our procedure.

ACKNOWLEDGMENTS

The main author expresses his thanks to Y. Todo, S. Pinches, and F. Zonca for crucial discussions about the applicability of the BB model to fast-particle modes. This work was performed within the frame of a cothesis agreement between the doctoral school of the Ecole Polytechnique, the Japan Atomic Energy Agency, and the Commissariat à l'Energie Atomique. It was supported by both the JAEA Foreign Researcher Inviting Program and the European Communities under the contract of Association between EURATOM and CEA. Two of the authors, M.L. and Y.I. are supported by the MEXT under Grant No. 22866086. The views and opinions expressed herein do not necessarily reflect those of the European Commission. Computations were performed on Altix3700 and BX900 systems at JAEA.

[1] R. Aymar, V. Chuyanov, M. Huguet, Y. Shimomura, The ITER Joint Central Team, and The ITER Home Teams, Nucl. Fusion **41**, 1301 (2001).
[2] C. Z. Cheng, L. Chen, and M. S. Chance, Ann. Phys. **161**, 21 (1985).
[3] A. Jaun, K. Appert, J. Vaclavik, and L. Villard, Comput. Phys. Commun. **92**, 153 (1995).
[4] A. Fukuyama and T. Akutsu, *Proceedings of the 19th IAEA Fusion Energy Conference*, Lyon, 2002 (IAEA, Vienna, 2003), Vol. TH/P3-14, pp. 1–5.
[5] C. Z. Cheng, Phys. Rep. **211**, 1 (1992).
[6] D. Borba, H. L. Berk, B. N. Breizman, A. Fasoli, F. Nabais, S. D. Pinches, S. E. Sharapov, D. Testa, and The EFDA-JET Workprogramme, Nucl. Fusion **42**, 1029 (2002).
[7] J. Candy, D. Borba, H. L. Berk, G. T. A. Huysmans, and W. Kerner, Phys. Plasmas **4**, 2597 (1997).
[8] S. D. Pinches, L. C. Appel, J. Candy, S. E. Sharapov, H. L. Berk, D. Borba, B. N. Breizman, T. C. Hender, K. I. Hopcraft, G. T. A. Huysmans, and W. Kerner, Comput. Phys. Commun. **111**, 133 (1998).
[9] A. Fasoli, D. Borba, G. Bosia, D. J. Campbell, J. A. Dobbing, C. Gormezano, J. Jacquinot, P. Lavanchy, J. B. Lister, P. Marmillod, J.-M. Moret, A. Santagiustina, and S. Sharapov, Phys. Rev. Lett. **75**, 645 (1995).

[10]A. Fasoli, D. Borba, B. Breizman, C. Gormezano, R. F. Heeter, A. Juan, M. Mantsinen, S. Sharapov, and D. Testa, Phys. Plasmas **7**, 1816 (2000).
[11]H. L. Berk, B. N. Breizman, and M. S. Pekker, Plasma Phys. Rep. **23**, 778 (1997).
[12]B. N. Breizman, H. L. Berk, M. S. Pekker, F. Porcelli, G. V. Stupakov, and K. L. Wong, Phys. Plasmas **4**, 1559 (1997).
[13]H. V. Wong and H. L. Berk, Phys. Plasmas **5**, 2781 (1998).
[14]X. Garbet, G. Dif-Pradalier, C. Nguyen, P. Angelino, Y. Sarazin, V. Grandgirard, P. Ghendrih, and A. Samain, in *Proceedings of AIP Conference on Theory of Fusion Plasmas*, edited by O. Sauter, X. Garbet, and E. Sindoni (AIP, Melville, NY, 2008), Vol. 1069, pp. 271–276.
[15]H. L. Berk, B. N. Breizman, and M. Pekker, Phys. Rev. Lett. **76**, 1256 (1996).
[16]S. D. Pinches, H. L. Berk, M. P. Gryaznevich, S. E. Sharapov, and The JET-EFDA Contributors, Plasma Phys. Controlled Fusion **46**, S47 (2004).
[17]A. Fasoli, B. N. Breizman, D. Borba, R. F. Heeter, M. S. Pekker, and S. E. Sharapov, Phys. Rev. Lett. **81**, 5564 (1998).
[18]R. F. Heeter, A. F. Fasoli, and S. E. Sharapov, Phys. Rev. Lett. **85**, 3177 (2000).
[19]Y. Kusama, G. J. Kramer, H. Kimura, M. Saigusa, T. Ozeki, K. Tobita, T. Oikawa, K. Shinohara, T. Kondoh, M. Moriyama, F. V. Tchernychev, M. Nemoto, A. Morioka, M. Iwase, N. Isei, T. Fujita, S. Takeji, M. Kuriyama, R. Nazikian, G. Y. Fu, K. W. Hill, and C. Z. Cheng, Nucl. Fusion **39**, 1837 (1999).
[20]W. W. Heidbrink, Plasma Phys. Controlled Fusion **37**, 937 (1995).
[21]K. G. McClements, M. P. Gryaznevich, S. E. Sharapov, R. J. Akers, L. C. Appel, G. F. Counsell, C. M. Roach, and R. Majeski, Plasma Phys. Controlled Fusion **41**, 661 (1999).
[22]E. D. Fredrickson, N. N. Gorelenkov, and H. L. Berk, Bull. Am. Phys. Soc. **51**(181), 181 (2006).
[23]M. Takechi, K. Toi, S. Takagi, G. Matsunaga, K. Ohkuni, S. Ohdachi, R. Akiyama, D. S. Darrow, A. Fujisawa, M. Gotoh, H. Idei, H. Iguchi, M. Isobe, T. Kondo, M. Kojima, S. Kubo, S. Lee, T. Minami, S. Morita, K. Matsuoka, S. Nishimura, S. Okamura, M. Osakabe, M. Sasao, M. Shimizu, C. Takahashi, K. Tanaka, and Y. Yoshimura, Phys. Rev. Lett. **83**, 312 (1999).
[24]M. Osakabe, S. Yamamoto, K. Toi, Y. Takeiri, S. Sakakibara, K. Nagaoka, K. Tanaka, K. Narihara, and The LHD Experimental Group, Nucl. Fusion **46**(10), S911 (2006).
[25]H. L. Berk, B. N. Breizman, and N. V. Petviashvili, Phys. Lett. A **234**, 213 (1997).
[26]M. Lesur, Y. Idomura, and X. Garbet, Phys. Plasmas **16**, 092305 (2009).
[27]B. Breizman, H. Berk, and H. Ye, Phys. Fluids B **5**, 3217 (1993).
[28]H. L. Berk, B. N. Breizman, and M. Pekker, Phys. Plasmas **2**, 3007 (1995).
[29]P. Bhatnagar, E. Gross, and M. Krook, Phys. Rev. **94**, 511 (1954).
[30]M. K. Lilley, B. N. Breizman, and S. E. Sharapov, Phys. Rev. Lett. **102**, 195003 (2009).
[31]I. B. Bernstein, J. M. Greene, and M. D. Kruskal, Phys. Rev. **108**, 546 (1957).
[32]K. Shinohara, Y. Kusama, M. Takechi, A. Morioka, M. Ishikawa, N. Oyama, K. Tobita, T. Ozeki, S. Takeji, S. Moriyama, T. Fujita, T. Oikawa, T. Suzuki, T. Nishitani, T. Kondoh, S. Lee, M. Kuriyama, JT-60 Team, G. J. Kramer, N. N. Gorelenkov, R. Nazikian, C. Z. Cheng, G. Y. Fu, and A. Fukuyama, Nucl. Fusion **41**, 603 (2001).
[33]K. Shinohara, M. Takechi, M. Ishikawa, Y. Kusama, A. Morioka, N. Oyama, K. Tobita, T. Ozeki, JT-60 Team, N. N. Gorelenkov, C. Z. Cheng, G. J. Kramer, and R. Nazikian, Nucl. Fusion **42**, 942 (2002).
[34]S. Briguglio, G. Fogaccia, G. Vlad, F. Zonca, K. Shinohara, M. Ishikawa, and M. Takechi, Phys. Plasmas **14**, 055904 (2007).
[35]P. Helander and D. J. Sigmar, in *Collisional Transport in Magnetized Plasmas*, edited by P. Helander and D. J. Sigmar (Press Syndicate of the University of Cambridge, Cambridge, 2002).
[36]N. Gorelenkov, S. Bernabei, C. Cheng, K. Hill, R. Nazikian, S. Kaye, Y. Kusama, G. Kramer, K. Shinohara, T. Ozeki, and M. Gorelenkova, Nucl. Fusion **40**, 1311 (2000).